

See discussions, stats, and author profiles for this publication at: <https://www.researchgate.net/publication/236668273>

Surface-Enhanced Infrared Spectroscopic Study of a CO-Covered Pt Electrode in Room-Temperature Ionic Liquid

ARTICLE in JOURNAL OF PHYSICAL CHEMISTRY LETTERS · APRIL 2013

Impact Factor: 7.46 · DOI: 10.1021/jz400657t

CITATIONS

8

READS

21

4 AUTHORS, INCLUDING:



Yao-Yue Yang

Southwest University for Nationalities

10 PUBLICATIONS 124 CITATIONS

SEE PROFILE



Wen-Bin Cai

Fudan University

111 PUBLICATIONS 2,115 CITATIONS

SEE PROFILE

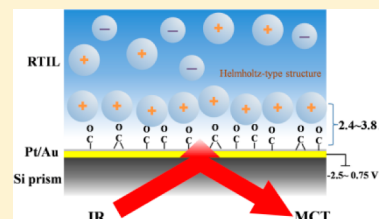
Surface-Enhanced Infrared Spectroscopic Study of a CO-Covered Pt Electrode in Room-Temperature Ionic Liquid

Yao-Yue Yang,[†] Li-Na Zhang,^{†,§} Masatoshi Osawa,[‡] and Wen-Bin Cai^{*,†}[†]Shanghai Key Laboratory of Molecular Catalysis and Innovative Materials, Collaborative Innovation Center of Chemistry for Energy Materials, Department of Chemistry, Fudan University, Shanghai 200433, China[‡]Catalysis Research Center, Hokkaido University, Sapporo 001-0021, Japan

S Supporting Information

ABSTRACT: ATR-SEIRAS is extended for the first time to study potential-induced surface and interface structure variation of a CO-covered Pt electrode in a room-temperature ionic liquid of *N*-butyl-*N*-methyl-piperidinium bis((trifluoromethyl)sulfonyl)imide (or [Pip₁₄][TNF₂]). Owing to a wide effective potential window of [Pip₁₄][TNF₂], a gradual conversion from bridged CO_{ad} (CO_B) to terminal CO_{ad} (CO_L) is observed in response to positively going potentials, suggesting that [Pip₁₄]⁺ may be involved in a strong electrostatic interaction with the CO_{ad}. This site conversion enables the ratio of the apparent absorption coefficient of CO_L to that of CO_B to be determined. Also, the spectral results reveal the potential-dependent CO_{ad} frequency variations as well as the potential-induced interfacial ionic reorientation and movement at the Pt/CO/[Pip₁₄][TNF₂] interface.

SECTION: Surfaces, Interfaces, Porous Materials, and Catalysis



Understanding the influence of surface electrostatic environment inclusive of electrode potential, solvent, and electrolyte on surface adsorbate as well as the double-layer structure is an everlasting fundamental topic in physical electrochemistry. To that end, CO adsorbed on Pt in electrochemical environment is the most frequently used model system. In line with this, in situ surface infrared spectroscopy has been intensively employed to the study of CO-covered Pt electrode/aqueous solution interfaces.^{1–4} However, the electrolysis of water and the CO electro-oxidation make it impossible to study CO adsorption over a wide potential range. To address this issue, several relevant investigations in organic solvents containing tetraalkylammonium or alkali-metal salts have been published, with an effective potential window extended up to 3.5 V.^{5–8} It was found that the spectral features of CO at Pt electrode/nonaqueous interfaces were virtually independent of the sorts of solvents and anions,⁶ whereas the CO Stark tuning rate decreased with the increase in cation's size.⁸ In addition, the electrolyte concentration had negligible effects on the CO Stark tuning rate based on previous investigations. However, the limited solubility of most salts in common organic solvents may prevent a reliable conclusion regarding the ionic effect from being drawn.

Room temperature ionic liquids (RTILs) merit high ionic concentrations, simple compositions, wide electrochemical window, and may serve simultaneously as solvents and supporting electrolytes.^{9–11} Hence, they provide an unprecedented opportunity for exploring the influence of highly concentrated cations on the interfacial behavior of CO adsorbed on Pt electrode. Furthermore, RTILs are promising green electrolytes for novel fuel cells^{12–14} and CO₂ electro-

reduction,¹⁵ where CO_{ad} species may act as a key poisoning intermediate. Therefore, the study of CO adsorption at metal electrodes in RTILs is also of practical interest for the development of novel energy and environment technologies.

Baldelli's group^{11,16,17} pioneered the investigation of a CO-covered Pt electrode in an imidazole-based RTIL using electrochemical sum frequency generation vibrational spectroscopy (SFG) with a focus on the double-layer thickness based on the analysis over 1900–2150 cm^{−1} spectral range. Nevertheless, the SFG measurement did not reveal potential-dependent sites conversion of CO_{ad} and dynamic ionic movement at CO/Pt electrode in RTIL because of the narrow spectral range that can be accessed in a set of experiment and the low S/N ratio. Fortunately, these problems can be effectively overcome by using high-sensitivity and broad-frequency surface-enhanced infrared absorption spectroscopy (SEIRAS) in ATR mode.^{18–22} So far, ATR-SEIRAS has been used to explore surface orientation^{19,20,22} and transport²¹ of the component ions of an RTIL per se on Au electrodes, but no reports exist on CO adsorption at Pt electrode in RTILs.

We initially report the potential-dependent adsorption behavior of CO_{ad} and variation of double-layer structure at a Pt electrode in a RTIL of *N*-butyl-*N*-methyl-piperidinium bis((trifluoromethyl)sulfonyl)imide (denoted hereafter as [Pip₁₄][TNF₂]; its structure is shown in Scheme S1 in the Supporting Information) by using in situ ATR-SEIRAS.

In situ electrochemical ATR-SEIRAS spectra for CO adsorbed at the Pt electrode are presented in Figure 1 (also

Received: March 26, 2013

Accepted: April 22, 2013

Published: April 22, 2013



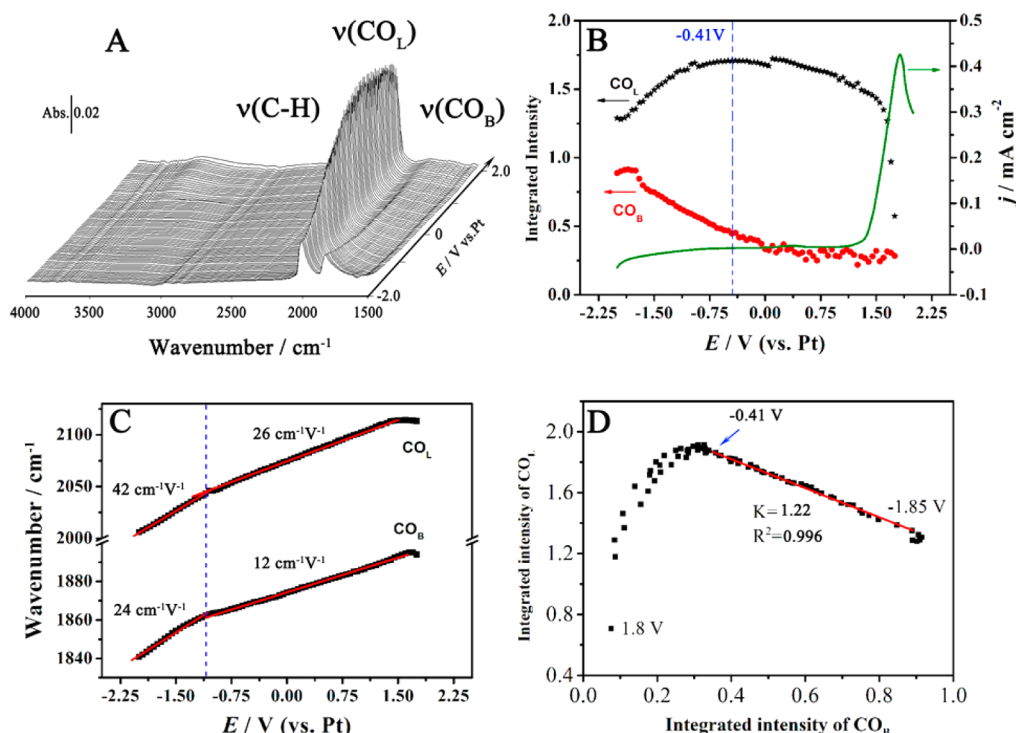


Figure 1. (A) In situ ATR-SEIRA spectra of CO adsorbed at a Pt film electrode in [Pip₁₄][TNF₂], calculated with the reference spectrum taken at -2.0 V before CO adsorption. Plots of potential-dependent (B) integrated intensities and (C) band frequencies for CO_L and CO_B. (D) Replot of integrated intensity of the CO_L band (I_L) versus that of the CO_B band (I_B). The olive line in panel B is the linear sweep voltammogram of a CO-predeposited Pt film electrode in [Pip₁₄][TNF₂] at 10 mV s⁻¹ from an initial potential of -2.0 V.

in Figure S1 in the Supporting Information with selected expanded spectra). The bands at 1840–1900 and 2000–2130 cm⁻¹ correspond to bridge-bonded CO (CO_B) and linearly bonded CO (CO_L), respectively, resembling those obtained in aqueous media (usually ca. 2060–2090 cm⁻¹ for CO_L, ca. 1800–1860 cm⁻¹ for CO_B) and organic solvents (ca. 2073–2102 cm⁻¹ for CO_L, ca. 1805–1861 cm⁻¹ for CO_B).^{2,3,7,23,24} The much larger range of CO_{ad} frequency variation concurring with the wider potential window (ca. 4.0 V) of Pt in RTILs favors a clear observation of CO adsorption site transition and a reliable evaluation of the apparent absorption coefficient of CO_L relative to that of CO_B. Notably, the previous SFG measurements did not show any potential induced variation of the CO_B band for Pt electrode in RTILs, probably due to fewer bridging sites on the Pt surfaces for SFG and a lower S/N ratio in the spectra.

At the Pt electrode/nonaqueous interface, it was once concluded that the site conversion from CO_L to CO_B with negatively going potential should occur in organic solvents containing alkali-metal cations but not those containing tetraalkylammonium ions.⁸ The main reason was explained in terms of the fact that more energy was required to overcome the solvation effects for the latter. Nevertheless, as shown in Figure 1A,B, in our case, the CO_L band diminishes, accompanied by the increase in the CO_B band when the potential is more negative than ca. -0.4 V, well below the onset oxidation potential. In other words, the site occupancy conversion from CO_L to CO_B may occur at the Pt electrode in an RTIL containing [Pip₁₄]⁺, which is basically a sort of tetraalkylammonium cation. Thereby, the potential-induced site conversion appears to be a general process for CO_{ad} at Pt surface. The failure of observing such a site conversion previously may be attributed at least partially to a limited

solubility and a strong solvation of the tetraalkylammonium cations in organic solvents. In an RTIL, the solvation of cations does not exist, and the electrostatic interaction between anions and cations is to some extent disrupted because the anions are largely expelled from the double layer of the CO-covered Pt electrode/[Pip₁₄][TNF₂] interface as potentials go negative of pzc (vide infra). The essentially “bare” interfacial [Pip₁₄]⁺ cations may proceed a specific electrostatic interaction with the underlying CO adlayer on Pt, similar to the desolvated alkali-metal cations in organic solvents⁸ (i.e., Pt-CO + [Pip₁₄]⁺ ⇌ Pt-CO...[Pip₁₄]⁺). This short-range interaction may induce the negative charge on the CO_{ad} species to yield a greater Pt-CO back-donation that would increase the stability of CO_B species and shift down the CO_{ad} band frequency.²⁶ The increased stability of CO_B species leads to a conversion from CO_L to CO_B (Figure 1B,D), whereas the frequency downshift induces a larger potential-dependent frequency shift (denoted as $\delta\nu/\delta E$) at more negative potentials, in qualitative agreement with Anderson’s theoretical prediction.²⁷ It may be necessary to point out that although the residual H₂O (<10 ppm) in the RTIL may be involved in electro-oxidizing CO at very high potentials (>1.35 V), this low level of water may not impact significantly the final results obtained as well as relevant interpretations in the double-layer region. One piece of evidence in line with this statement is that we could not see a sharp $\nu(\text{OH})$ band at ca. 3650 cm⁻¹ due to so-called “free water” molecules on top of CO adlayer.²

The ready observation of the CO occupancy site conversion over a rather wide potential range enables the more reliable and accurate determination of the ratio of the apparent absorption coefficient of CO_L relative to that of CO_B (α_L/α_B). Here we use the concept of “apparent absorption coefficient” instead of “absorption coefficient” to include the dipole–dipole coupling

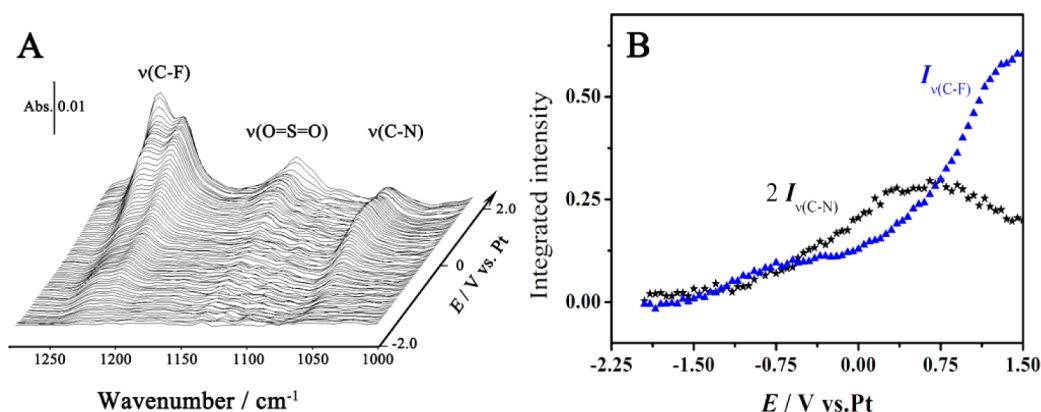


Figure 2. (A) In situ ATR-SEIRA spectra of CO-adsorbed Pt electrode in $[\text{Pip}_{14}][\text{TNF}_2]$ over the frequency range from 1300 to 1000 cm^{-1} ; all conditions are the same as those in Figure 1A. (B) Plots of the $\nu(\text{C-N})$ and $\nu(\text{C-F})$ band intensities as a function of electrode potential.

effect. (For more discussions, please see the Supporting Information.) In other words, at a constant total coverage of CO_{ad} (θ_{total}), the integrated band intensities of CO_L (I_L) and CO_B (I_B) are assumed to run a linearity with their respective coverage (θ), that is, $I_L = \alpha_L \theta_L$ and $I_B = \alpha_B \theta_B$. Thus, an equation can be obtained as $(I_L/\alpha_L) + (I_B/\alpha_B) = C$, namely, $I_L = C\alpha_L - (\alpha_L/\alpha_B)I_B$. Strictly speaking, these equations are only correct if α_L and α_B depend exclusively on θ_{total} and not on θ_L and θ_B . Consequently, linear plot of I_L versus I_B may be expected only within a limited range of variations of θ_L and θ_B (correspondingly within a certain potential range), where α_L and α_B are virtually independent of θ_L and θ_B , respectively. In Figure 1D, the linear plot of I_L versus I_B over a range of -1.85 to -0.4 V yields α_L/α_B to be ca. 1.2, close to that obtained for a low-coverage CO adlayer ($\theta_{\text{total}} = 0.04$) on Ni(100) electrode (ca. 1.1) in aqueous solutions,²⁸ largely regardless of the total CO coverage and the surrounding chemical nature. The slope change of the I_L versus I_B plot at potentials positive of ca. -0.4 V may be attributed to the nonlinearity of I_L with θ_L and I_B with θ_B . In addition, the uncertainty in estimating the weak CO_B band intensity results in the scattering of data points.

Besides the site conversion, the potential-dependent frequency shift of CO (for simplicity, we here focus on the CO_L band) also reflects to some extent the variation of electric double-layer structure. Note that three controversial models (i. e., the Helmholtz model, the Gouy–Chapman model, and the multilayer model) or their combinations have been proposed in the description of the ionic liquid/metal interface.¹¹ Baldelli and coworkers¹⁷ suggested that ions organize in a Helmholtz-type layer at ionic liquid/metal interface according to their SFG investigation, as described above. In our case, as shown in Figure 1C, two linear sections can be visualized in the plots of potential-dependent frequency shift with a transition region around -1.0 V, and the two slopes ($\delta\nu/\delta E$) of 42 and 26 $\text{cm}^{-1} \text{V}^{-1}$ for CO_L (also 24 and 12 $\text{cm}^{-1} \text{V}^{-1}$ for CO_B) correspond to lower and higher potential regions, respectively. This transition may be qualitatively understood according to the above specific electrostatic interaction based on the charge-transfer model. However, more straightforward evidence is needed to answer why the transition occurs around -1.0 V, although we did observe a deflection of the double-layer current at ca. -1.0 V in the voltammetric profile of Pt electrode in the RTIL in the absence of CO adsorption. (See Figure S2 in the Supporting Information.) Presumably, an interfacial ionic rearrangement occurs to favor a shorter-range interaction between the CO_{ads}

and the $[\text{Pip}_{14}]^+$ cations (and thus a stronger and more effective Pt-CO back-donation) at the more negative potential region.

In addition to the above “charge-transfer” model, the alternative “Stark effect” model is also commonly used to understand the potential-dependent variation of the CO frequency at a fixed CO coverage.²⁵ According to the “Stark effect” model, $\delta\nu/\delta E$ can be considered due to the potential drop between the electrode and the charge center of the ion layer by assuming a Helmholtz-type double-layer structure. Along this line, the distance from the Pt surface to the charge center of the innermost cation layer (for more details, see the Supporting Information), d_H , may be approximately evaluated according to the equation $d_H = (\text{d}\nu(\text{CO}_L)/\text{d}E^*)/(\text{d}\nu(\text{CO}_L)/\text{d}E)$, where the local electric field Stark effect $\text{d}\nu(\text{CO}_L)/\text{d}E^*$ is assumed to be ca. $1 \times 10^{-6} \text{ cm}^{-1}/(\text{V}/\text{cm})$.²⁹ Thereby, the resulting d_H is ~ 2.4 Å for $E < \text{ca. } -1.0$ V and 3.8 Å for $E > \text{ca. } -1.0$ V. Notably, the d_H values are only an approximation but may serve as an indicator of the interfacial structure change at the Pt/CO/RTIL interface. The apparently smaller d_H value for $E < \text{ca. } -1.0$ V reflects a significantly increased portion of more tightly adsorbed CO_B species in the CO adlayer (see Figure 1A), noting that the calculation is based on the Stark tuning rate and the local electric field Stark effect of CO_L . Cooperatively, the two estimates of d_H agree qualitatively with the potential-dependent calculation results based on the “charge-transfer” model by Anderson and coworkers, who showed that $d_{\text{CO}(L)}$ and $d_{\text{CO}(B)}$ are about 2.1 and 1.7 Å, respectively, and decrease with decreasing potential at different paces.²⁷ In other words, the simple Helmholtz-type model seems to some extent effective to address the current Pt/CO/RTIL interfacial change.^{11,17} Furthermore, the present infrared results show the potential-induced variation of d_H at molecular level, which was not previously observed by using SFG.^{17,30}

The potential of zero charge (pzc) of a CO-covered Pt electrode should be estimated at first to discuss the potential-dependent adsorption/desorption of certain ions in the double layer. Weaver^{7,26} calculated the pzc values for the Pt(110)/CO in aqueous solutions and Pt(110)/CO and Pt(111)/CO in nonaqueous solutions to be around 0.8, 0.8, and 1.0 ± 0.2 V (vs SCE), respectively, suggesting that the influence of the solvent upon pzc for CO-covered Pt electrode is weak and nonspecific. Later, Cuesta et al.³¹ obtained an excellent agreement between their experiment results and Weaver’s estimation though a CO displacement method. Thereby, in our case, we roughly assume that the pzc value lies around 0.7 ± 0.2 V (vs Pt). (Note that

the Pt quasi-reference electrode has a 0.12 ± 0.005 V potential difference with SCE in $[\text{Pip}_{14}][\text{TNf}_2]$; see Figure S3 in the Supporting Information.).

At a CO-covered Pt surface, the potential-induced movements of interfacial $[\text{Pip}_{14}]^+$ cations and $[\text{TNf}_2]^-$ anions could be addressed by analyzing the ATR-SEIRA spectra in Figure 2. Notably, the intensity of $\nu(\text{C}-\text{N})$ band is much higher than that of $\nu(\text{C}-\text{H})$ band, and the $\nu(\text{O}=\text{S}=\text{O})$ band runs parallel to the $\nu(\text{C}-\text{F})$ band as a function of potential; thus we used the $\nu(\text{C}-\text{N})$ band (from the cations) and the $\nu(\text{C}-\text{F})$ band (from the anions) as indicators to obtain a reliable results. For the potentials lower than 0.75 V (around pzc), the $\nu(\text{C}-\text{N})$ ($1024\text{--}1080\text{ cm}^{-1}$) band intensity due to $[\text{Pip}_{14}]^+$ augments with increasing potential and gets the maximum at ca. 0.75 V. Because the band intensity is essentially proportional to the coverage of a surface (or near-surface) species as well as the square of the vertical component of the transition dipole moment, we may deduce that the piperidine ring of $[\text{Pip}_{14}]^+$ reorients from a parallel configuration to a tilted one (rather than the increased surface cation concentration) as the potential increases. Similar potential-induced reorientation was proposed for the imidazole ring at Au- or Pt/imidazole-based RTIL interfaces using conventional FTIR and SFG in the absence of CO adsorption.^{19,20,30} Meanwhile, the $\nu(\text{C}-\text{F})$ ($1180\text{--}1280\text{ cm}^{-1}$) band intensity due to $[\text{TNf}_2]^-$ increases monotonously, indicating that the anions near the innermost layer of cations increase statistically with increasing potential. This observation agrees with the fact that the positive shift of the electrode potential favors the anions to approach the electrode surface. When the potential goes positive of ca. 0.75 V, $\nu(\text{C}-\text{N})$ ($1024\text{--}1080\text{ cm}^{-1}$) band intensity gradually diminishes as a result of the desorption of cations at positive potentials, while the $\nu(\text{C}-\text{F})$ band intensity increases sharply owing to the adsorptive enrichment of $[\text{TNf}_2]^-$ to form the Helmholtz-type layer on CO-covered Pt electrode.

In summary, in situ ATR-SEIRAS is extended to probe the CO-covered Pt electrode/RTIL interface for the first time. High-quality SEIRA spectra over a wide potential window benefit the study of potential-dependent CO site conversion and dynamic ionic variation at the electric double layer, revealing different surface and interfacial behaviors from those for CO-covered electrodes in aqueous and nonaqueous electrolytes.

EXPERIMENTAL SECTION

The Pt electrode was prepared by the so-called “two-step wet process” in which a Au underlayer was chemically deposited on the basal plane of a hemicylindrical Si prism, followed by electrodeposition of a sufficiently thick pinhole-free Pt overfilm in a homemade spectroelectrochemical cell.² The as-prepared Pt electrode was electrochemically cleaned in 0.1 M HClO_4 and then thoroughly rinsed by a copious amount of ultrapure Milli-Q water (Millipore, $\geq 18.2\text{ M}\Omega\cdot\text{cm}$). After sparging the empty cell with high-purity N_2 at a high flow rate for at least 1 h, water-removed hydrophobic RTIL $[\text{Pip}_{14}^+][\text{TNf}_2^-]$ (Lanzhou Chemical Physics Research Institute, Lanzhou, China; halides $<10\text{ ppm}$, water $<10\text{ ppm}$) was quickly injected under the protection of high-purity N_2 . (It was absorbed by molecule sieves (4 Å) and successively kept under vacuum at $70\text{--}80^\circ\text{C}$ for several hours to minimize the water content in $[\text{Pip}_{14}^+][\text{TNf}_2^-]$.)¹⁰ Eventually, electrochemical ATR-SEIRAS in $[\text{Pip}_{14}^+][\text{TNf}_2^-]$ was carried out, similar to that in aqueous media.² The CO preadsorbed Pt film electrode was obtained by

first introducing high-purity CO for ca. 30 min, then sparging N_2 for ca. 1 h at -1.8 V (vs Pt). All spectra are shown in the absorbance unit defined as $A = -\log(I/I_0)$, where I and I_0 represent the intensities of the reflected radiation at the sample and reference potentials, respectively. A Varian 3100 FT-IR spectrometer (Varian, CA) equipped with an MCT detector was used for IR measurements, a CHI 660B electrochemistry workstation (Shanghai CH Instruments, China) was employed for potential control, and a Pt wire and a Pt sheet served as the quasi-reference and counter electrodes, respectively.

ASSOCIATED CONTENT

Supporting Information

Structure of $[\text{Pip}_{14}][\text{TNf}_2]$; scheme of experimental procedures and technical background of ATR-SEIRAS; expanded ATR-SEIRA spectra; CVs for a bare and a CO-covered Pt electrode in RTIL; potential difference of Pt vs SCE in the RTIL; discussions on the obtainment of the ratio of apparent absorption coefficients, potential dependent frequency shifts, and interfacial structural changes. This material is available free of charge via the Internet at <http://pubs.acs.org>.

AUTHOR INFORMATION

Corresponding Author

*E-mail: wbcail@fudan.edu.cn.

Present Address

[§]L.-N.Z.: Guohong Memorial Middle School, Foshan 528312, Guangdong Province, China.

Notes

The authors declare no competing financial interest.

ACKNOWLEDGMENTS

This work is supported by NSFC (nos. 21073045 and 21273046), SMCST (nos. 11JC140200 and 08DZ2270500).

REFERENCES

- (1) Bjerke, A. E.; Griffiths, P. R.; Theiss, W. Surface-Enhanced Infrared Absorption of CO on Platinized Platinum. *Anal. Chem.* **1999**, *71*, 1967–1974.
- (2) Yan, Y. G.; Yang, Y. Y.; Peng, B.; Malkhandi, S.; Bund, A.; Stimming, U.; Cai, W. B. Study of CO Oxidation on Polycrystalline Pt Electrodes in Acidic Solution by ATR-SEIRAS. *J. Phys. Chem. C* **2011**, *115*, 16378–16388.
- (3) Samjeske, G.; Komatsu, K.; Osawa, M. Dynamics of CO Oxidation on a Polycrystalline Platinum Electrode: A Time-Resolved Infrared Study. *J. Phys. Chem. C* **2009**, *113*, 10222–10228.
- (4) Yajima, T.; Uchida, H.; Watanabe, M. In-situ ATR-FTIR Spectroscopic Study of Electro-oxidation of Methanol and Adsorbed CO at Pt-Ru Alloy. *J. Phys. Chem. B* **2004**, *108*, 2654–2659.
- (5) Roth, J. D.; Chang, S. C.; Weaver, M. J. Infrared-Spectroscopy of Carbon-Monoxide Electrosorption on Platinum over Wide Potential Ranges - Delineation of Site Occupancy Changes and Nonlinear Band Frequency Potential Shifts. *J. Electroanal. Chem.* **1990**, *288*, 285–292.
- (6) Chang, S. C.; Jiang, X.; Roth, J. D.; Weaver, M. J. Influence of Potential on Metal-Adsorbate Structure - Solvent-Independent Nature of Infrared-Spectra for Pt(111)/CO. *J. Phys. Chem.* **1991**, *95*, 5378–5382.
- (7) Jiang, X. D.; Weaver, M. J. The Role of Interfacial Potential in Adsorbate Bonding - Electrode Potential-Dependent Infrared-Spectra for Saturated CO Adlayers on Pt(110) and Related Electrochemical Surfaces in Varying Solvent Environments. *Surf. Sci.* **1992**, *275*, 237–252.
- (8) Roth, J. D.; Weaver, M. J. Role of the Double-Layer Cation on the Potential-Dependent Stretching Frequencies and Binding Geo-

metries of Carbon-Monoxide at Platinum Nonaqueous Interfaces. *Langmuir* **1992**, *8*, 1451–1458.

(9) Buzzeo, M. C.; Evans, R. G.; Compton, R. G. Non-Haloaluminate Room-temperature Ionic Liquids in Electrochemistry - A Review. *ChemPhysChem* **2004**, *5*, 1106–1120.

(10) Su, Y. Z.; Fu, Y. C.; Wei, Y. M.; Yan, J. W.; Mao, B. W. The Electrode/Ionic Liquid Interface: Electric Double Layer and Metal Electrodeposition. *ChemPhysChem* **2010**, *11*, 2764–2778.

(11) Baldelli, S. Surface Structure at the Ionic Liquid-electrified Metal Interface. *Acc. Chem. Res.* **2008**, *41*, 421–431.

(12) Ejigu, A.; Johnson, L.; Licence, P.; Walsh, D. A. Electrocatalytic Oxidation of Methanol and Carbon Monoxide at Platinum in Protic Ionic Liquids. *Electrochem. Commun.* **2012**, *23*, 122–124.

(13) de Souza, R. F.; Padilha, J. C.; Goncalves, R. S.; Dupont, J. Room Temperature Dialkylimidazolium Ionic Liquid-based Fuel Cells. *Electrochem. Commun.* **2003**, *5*, 728–731.

(14) Gao, J.; Liu, J. G.; Liu, W. M.; Li, B.; Xin, Y. C.; Yin, Y.; Jungu; Zou, Z. G. Proton Exchange Membrane Fuel Cell Working at Elevated Temperature with Ionic Liquid as Electrolyte. *Int. J. Electrochem. Sc.* **2011**, *6*, 6115–6122.

(15) Rosen, B. A.; Salehi-Khojin, A.; Thorson, M. R.; Zhu, W.; Whipple, D. T.; Kenis, P. J. A.; Masel, R. I. Ionic Liquid-Mediated Selective Conversion of CO₂ to CO at Low Overpotentials. *Science* **2011**, *334*, 643–644.

(16) Baldelli, S. Probing Electric Fields at the Ionic Liquid-electrode Interface Using Sum Frequency Generation Spectroscopy and Electrochemistry. *J. Phys. Chem. B* **2005**, *109*, 13049–13051.

(17) Aliaga, C.; Santos, C. S.; Baldelli, S. Surface Chemistry of Room-temperature Ionic Liquids. *Phys. Chem. Chem. Phys.* **2007**, *9*, 3683–3700.

(18) Osawa, M. Dynamic Processes in Electrochemical Reactions Studied by Surface-Enhanced Infrared Absorption Spectroscopy (SEIRAS). *Bull. Chem. Soc. Jpn.* **1997**, *70*, 2861–2880.

(19) Nanbu, N.; Sasaki, Y.; Kitamura, F. In Situ FT-IR Spectroscopic Observation of a Room-temperature Molten Salt Vertical Bar Gold Electrode Interphase. *Electrochem. Commun.* **2003**, *5*, 383–387.

(20) Nanbu, N.; Kato, T.; Sasaki, Y.; Kitamura, F. In Situ SEIRAS Study of Room-Temperature Ionic Liquid Vertical Bar Gold Electrode Interphase. *Electrochemistry* **2005**, *73*, 610–613.

(21) Richey, F. W.; Elabd, Y. A. In Situ Molecular Level Measurements of Ion Dynamics in an Electrochemical Capacitor. *J. Phys. Chem. Lett.* **2012**, 3297–3301.

(22) Romann, T.; Oll, O.; Pikma, P.; Lust, E. Abnormal Infrared Effects on Bismuth Thin Film-EMIMBF₄ Ionic Liquid Interface. *Electrochem. Commun.* **2012**, *23*, 118–121.

(23) Chang, S. C.; Leung, L. W. H.; Weaver, M. J. Comparisons between Coverage-Dependent Infrared Frequencies for Carbon-Monoxide Adsorbed on Ordered Pt(111), Pt(100), and Pt(110) in Electrochemical and Ultrahigh-Vacuum Environments. *J. Phys. Chem.* **1989**, *93*, 5341–5345.

(24) Cuesta, A.; Couto, A.; Rincon, A.; Perez, M. C.; Lopez-Cudero, A.; Gutierrez, C. Potential Dependence of The Saturation CO Coverage of Pt Electrodes: The Origin of the Pre-Peak in CO-stripping Voltammograms. Part 3: Pt(poly). *J. Electroanal. Chem.* **2006**, *586*, 184–195.

(25) Nichols, R. J., IR Spectroscopy of Molecules at the Solid-Solution Interface. In *Adsorption of Molecules at Metal Electrodes*; Lipkowsky, J., Ross, P. N., Eds.; VCH Publishers: New York, 1992; pp 347–387.

(26) Anderson, M. R.; Huang, J. M. The Influence of Cation Size Upon the Infrared-Spectrum of Carbon-Monoxide Adsorbed on Platinum-Electrodes. *J. Electroanal. Chem.* **1991**, *318*, 335–347.

(27) Mehandru, S. P.; Anderson, A. B. Potential-Induced Variations in Properties for CO Adsorbed on a Platinum-Electrode. *J. Phys. Chem.* **1989**, *93*, 2044–2047.

(28) Yoshinobu, J.; Takagi, N.; Kawai, M. Site Conversion of CO on Ni(100) - Binding-Energy Difference and Role of Low-Energy Hindered Vibrations. *Chem. Phys. Lett.* **1993**, *211*, 48–52.

(29) Lambert, D. K. Vibrational Stark-Effect of Co on Ni(100), and Co in the Aqueous Double-Layer - Experiment, Theory, and Models. *J. Chem. Phys.* **1988**, *89*, 3847–3860.

(30) Aliaga, C.; Baldelli, S. Sum Frequency Generation Spectroscopy and Double-Layer Capacitance Studies of the 1-Butyl-3-methylimidazolium Dicyanamide-Platinum Interface. *J. Phys. Chem. B* **2006**, *110*, 18481–18491.

(31) Cuesta, A. Measurement of the Surface Charge Density of CO-saturated Pt(111) Electrodes as a Function of Potential: the Potential of Zero Charge of Pt(111). *Surf. Sci.* **2004**, *572*, 11–22.